Cocaine- and Amphetamine-Regulated Transcript Is a Potent Stimulator of GnRH and Kisspeptin Cells and May Contribute to Negative Energy Balance-induced Reproductive Inhibition in Females

Cadence True, Saurabh Verma, Kevin L. Grove, and M. Susan Smith

Divisions of Diabetes, Obesity, & Metabolism, and Neuroscience, Oregon National Primate Research Center, Oregon Health & Science University, Beaverton, Oregon 97006

Cocaine- and amphetamine-regulated transcript (CART) is a hypothalamic neuropeptide implicated in both metabolic and reproductive regulation, raising the possibility that CART plays a role in reproductive inhibition during negative metabolic conditions. The current study characterized CART's regulatory influence on GnRH and kisspeptin (Kiss1) cells and determined the sensitivity of different CART populations to negative energy balance. CART fibers made close appositions to 60% of GnRH cells, with the majority of the fibers (>80%) originating from the arcuate nucleus (ARH) CART/pro-opiomelanocortin population. Electrophysiological recordings in GnRH-green fluorescent protein rats demonstrated that CART postsynaptically depolarizes GnRH cells. CART fibers from the ARH were also observed in close contact with Kiss1 cells in the ARH and anteroventral periventricular nucleus (AVPV). Recordings in Kiss1-GFP mice demonstrated CART also postsynaptically depolarizes ARH Kiss1 cells, suggesting CART may act directly and indirectly, via Kiss1 populations, to stimulate GnRH neurons. CART protein and mRNA levels were analyzed in 2 models of negative energy balance: caloric restriction (CR) and lactation. Both CART mRNA levels and the number of CART-immunoreactive cells were suppressed in the ARH during CR but not during lactation. AVPV CART mRNA was suppressed during CR, but not during lactation when there was a dramatic increase in CART-immunoreactive cells. These data suggest differing regulatory signals of CART between the models. In conclusion, both morphological and electrophysiological methods identify CART as a novel and potent stimulator of Kiss1 and GnRH neurons and suppression of CART expression during negative metabolic conditions could contribute to inhibition of the reproductive axis. (***Endocrinology*** **154: 2821–2832, 2013)**

Negative metabolic states, from either undernutrition or overexertion, result in inhibition of the reproductive neuroendocrine hormones kisspeptin (Kiss1) and GnRH in all female mammals studied to date. This inhibition of Kiss1 and GnRH results in impaired reproductive function, but the pathways underlying this metabolically driven anovulatory state remain poorly understood. Although significant evidence exists for the permissive role of the adipocyte hormone leptin in signaling sufficient energy stores for pubertal maturation, conflicting evidence exists on the role of this hormone in mediating negative energy balance-induced GnRH inhibition during adulthood (1–4). Importantly, restoration of leptin to physiological levels has no effect to restore GnRH release or Kiss1 expression during negative energy balance in rats, indicating additional signals must contribute to the observed reproductive inhibition (1). Many of the hypothalamic feeding neuropeptides are also thought to modulate GnRH release, including cocaine- and amphetamine-regulated transcript (CART) (5).

ISSN Print 0013-7227 ISSN Online 1945-7170
Printed in U.S.A.

Received February 14, 2013. Accepted May 29, 2013.
First Published Online June 4, 2013

Abbreviations: aCSF, artificial cerebrospinal fluid; ARH, arcuate nucleus; AVPV, anteroventral periventricular nucleus; CART, cocaine- and amphetamine-regulated transcript; CR, caloric restriction; DMH, dorsomedial hypothalamus; EGFP, enhanced green fluorescent protein; GFP, green fluorescent protein; ir, immunoreactive; Kiss1, kisspeptin; OVX+E, ovariectomized + estradiol; POA, preoptic area; POMC, pro-opiomelanocortin; TTX, tetrodotoxin.

In metabolic circuits CART acts primarily as a satiety signal to decrease food intake and increase thermogenesis (6–9). CART may also play a role in reproduction based on previous results documenting CART fibers in close contact with GnRH cells (10, 11). Neuronal tracing studies have determined that CART cells in the arcuate nucleus (ARH), ventral premammillary nucleus, dorsomedial hypothalamus (DMH), and the anteroventral periventricular region (AVPV) all have projections to the region containing GnRH neurons (11). Although it has previously been demonstrated that ARH CART levels are inhibited during negative energy balance, it is unclear whether any of the additional hypothalamic CART populations are sensitive to negative metabolic states (8, 12, 13).

Previous work has demonstrated that CART can stimulate GnRH pulse frequency in a hypothalamic explant preparation; however, it remains unclear whether CART acts directly on GnRH neurons or through a presynaptic population to elicit this effect. One potential presynaptic mediator may be Kiss1, which potently stimulates GnRH release and is suppressed during conditions of negative energy balance (1, 14–20). No studies to date have examined the relationship between CART and Kiss1 and how this may contribute to negative energy balance-induced GnRH inhibition. The goal of the current study was to determine what if any effect CART has on GnRH and Kiss1 cells by using: 1) immunohistochemistry techniques to assess CART fibers in relationship to GnRH and Kiss1 cells and 2) electrophysiological recordings in GnRH-green fluorescent protein (GFP) rats and Kiss1-GFP mice to determine effects on cell firing. 3) Finally, we investigated whether CART populations, specifically those previously shown to make projections to the area of GnRH neurons, are sensitive to conditions of negative energy balance and thus could provide a mechanism by which negative metabolic conditions are relayed to reproductive circuits.

Materials and Methods

Animals

All protocols were approved by the Oregon Health and Science University Institutional Animal Care and Use Committee and conducted in accordance with NIH Guidelines for Care and Use of Laboratory Animals. For all studies animals were maintained on a 12-hour light (0600) and dark (1800) cycle throughout the experiment and allowed water ad libitum. For histological experiments examining ARH and AVPV Kiss1, cells adult female Wistar rats (Simonsen, Gilroy, California) were used. For histological experiments examining GnRH cells and electrophysiological recordings, transgenic Wistar rats expressing the enhanced green fluorescent protein (EGFP) under the control of the GnRH promoter were used (21). All female rats were ovariectomized and subcutaneously implanted with silastic implants (1 cm/100 g of body weight) containing 30 μg/mL estradiol in oil (ovariectomized + estradiol [OVX+E]) resulting in low basal levels of serum estradiol (1, 22).

To investigate the effects of CART on Kiss1 cell firing female Kiss1-CreGFP mice (a generous gift from Dr Robert Steiner, University of Washington [23]) were used. Although there may be species differences between mice and rats, electrophysiological recordings of GnRH neurons and their electrophysiological response to Kiss1 appear identical between these species (unpublished data). For maximum expression of ARH Kiss1, females were OVX (24) as described above but did not receive hormone replacement.

Experiments 1 and 4. Morphological interactions of CART, Kiss1, and GnRH, and CART expression during negative energy balance

Lactation and caloric restriction models

Both the lactation and the caloric restriction (CR) models have been described previously (1, 25). For the lactation studies, on day 2 postpartum litters were adjusted to 8 pups and the animals were OVX+E. For the corresponding controls, animals were OVX+E on a random day of the estrous cycle. Both groups were euthanized 8/9 days after OVX+E, corresponding to day 10/11 postpartum. For CR studies, animals were OVX+E on a random day of the cycle and 4 days later were placed into either the ad libitum fed control group or the 50% CR group. Food intake was measured; body weights were recorded, and food was given to the CR group between 0700 and 0800 hours every morning. Both groups were killed 16 days after OVX+E, corresponding to 12 days of CR.

Immunohistochemistry

Immunohistochemistry was performed as described previously (14). Animals were perfused transcardially with 0.9% saline and 4% paraformaldehyde (pH 7.4); brains were then frozen and cut into a 1-in-6 series of 25-μm sections. Primary antibodies and concentrations were as follows: rabbit anti-CART (Phoenix H-003–62, 1:500 000, Phoenix Pharmaceuticals, Inc, Burlingame, California), rabbit anti-Kisspeptin (Millipore AB9754, 1:1000, EMD Millipore Corporation, Billerica, Massachusetts), and sheep anti-α-MSH (Millipore AB5087, 1:5000). All 3 antibodies have previously been validated showing a lack of immunoreactive staining following preabsorption with the corresponding peptide (26–28). In addition, the observed immunoreactivity patterns in the current study were consistent with previously published corresponding mRNA for all 3 neuropeptides (8, 29, 30). The CART staining was performed first, and after overnight incubation in primary antibody at room temperature, a biotinylatedtyramide amplification was performed as described previously (31) using a biotinylated antirabbit antibody (Jackson Immunoresearch, 711–065-152, Jackson ImmunoResearch Laboratories, Inc, West Grove, Pennsylvania), A/B solution (Vector, PK-6200, Vector Laboratories Inc, Burlingame, California), and biotinylated tyramide (PerkinElmer, SAT7000, PerkinElmer, Waltham, Massachusetts). Finally tissue was incubated in Alexa Fluor 488 (or Alexa Fluor 568 for staining in GnRH-GFP tissue, Life Technologies, Grand Island, New York) conjugated to streptavidin (Invitrogen, Life Tech-

nologies, Carlsbad, California). For additional staining, tissue was rinsed in buffer for 2 hours followed by incubation in antikisspeptin and anti-α-MSH antibodies overnight at room temperature, followed by 1 hour in Alexa Fluor 568 antirabbit and donkey antisheep Cy5 secondary antibodies.

To avoid cross-reactivity of the 2 antibodies raised in the rabbit, the rabbit anti-CART antibody was used at 1:500 000 with tyramide concentration and followed sequentially by immunohistochemistry with rabbit anti-Kiss1. This concentration for the CART antibody resulted in a complete absence of staining with direct secondary detection. Additionally, when the entire double-labeled protocol was carried out with either the CART or the kisspeptin antibody omitted, there was a complete lack of staining in the given fluorophore channel, suggesting that there was little cross-reactivity of these antibodies. This concentration of the CART antibody resulted in abundant fiber staining in the ARH and DMH, consistent with previous descriptions of CART expression (32, 33).

In situ hybridization

In situ hybridization was performed as described previously (14, 25). Brains were collected by rapid decapitation and frozen on dry ice. Tissue was sectioned into a 1-in-3 series of 20-μM slices using a cryostat. The Kiss1 probe (a gift from the laboratory of Dr Robert Steiner, University of Washington), which has been characterized previously (34), was transcribed using a T7 polymerase in the presence of ^{33}P. The CART probe (a gift from Dr Joel Elmquist and Dr Carol Elias, University of Texas Southwestern Medical School) was transcribed using a T3 polymerase in the presence of ^{35}S. The Kiss1-^{33}P probe was used at a concentration of 4.5 million cpm/100 μL, whereas the CART-^{35}S probe was used at a concentration of 3.5 million cpm/100 μL. Slides were incubated in this diluted radioactive probe overnight in humidified chambers at 55°C (14, 25). For quantification of mRNA levels, in situ hybridization slides were dipped in Kodak NTB emulsion (Eastman Kodak, Rochester, New York) and developed for 6 and 9 days for the CART and Kiss probes, respectively.

Confocal analysis

All immunofluorescence analysis was performed on images taken with a Leica SP5 confocal microscope with Acousto-Optical Beam Splitter (Buffalo Grove, Illinois). For AVPV, DMH and ARH CART cell count analyses photomicrographs were taken with a ×20 objective at 512 × 512 pixel resolution and at a speed of 400 Hz. For each animal CART cell counts were bilaterally determined and reported as the total number of cells from 3 AVPV sections, 2 DMH sections, and 4 ARH sections per animal. For analysis of CART fiber close appositions to GnRH, AVPV Kiss1, and ARH Kiss1 cells, the methods used have been described previously (35–37). Photomicrographs were taken at a ×40 magnification at 1024 × 1024 pixel resolution and at a speed of 700 Hz. Focal planes were 1 μM apart for this analysis and 2 preoptic area (POA), 2 AVPV, and 3 ARH sections were analyzed per animal. Photomicrographs of the POA were taken to incorporate areas of highest GnRH cell density and 2 to 3 photomicrographs were taken across 2 sections to obtain analysis for 10 GnRH cells. For more abundant AVPV and ARH Kiss1 cells, all visible cells in confocal photomicrographs of 2 AVPV (bilateral) and 3 ARH sections (unilateral) were analyzed for contact analysis. Stacks were analyzed using ImageJ software and the Image5D plugin (developed by Joachim Walter, available at the ImageJ Developer Project). Image5D was also used to pseudocolor the GnRH-GFP channel red and the CART-immunoreactive (ir) channel green for consistency in presentation of contact analysis photomicrographs.

Silver grain analysis

Dark-field silver grain analysis was performed using Metamorph Imagining software (Molecular Devices, Sunnyvale, California). Pictures were taken at constant exposures, and a common threshold for silver grain detection was used for analysis at each nucleus. Integrated intensity was measured in a fixed region of interest for the ARH, AVPV, and DMH and in a nearby region lacking signal for subtraction of background levels. The integrated intensity was the mean averaged across 9 ARH sections, 4 AVPV sections, and 3 DMH sections per animal.

Experiments 2 and 3. CART effects on GnRH and ARH Kiss1 cell firing

Brain slice preparation

Rats or mice were transcardially perfused with ice-cold oxygenated cutting solution (composed of [in mM] 208 sucrose, 2 KCl, 1 $MgCl_2$, 1.25 NaH_2PO_4, 26 $NaHCO_3$, 2 $MgSO_4$, 1 $CaCl_2$, 10 HEPES, and 10 glucose, adjusted to pH 7.4 with NaOH, and was continuously aerated). Brains were quickly dissected and 250-μm hypothalamic slices were cut using a vibratome. Hypothalamic slices were incubated at 34°C in warm oxygenated artificial cerebrospinal fluid (aCSF) for 30 minutes and then stored at room temperature until used for recording. aCSF consisted of (in mM): 124 NaCl, 5 KCl, 2 $MgCl_2$, 2.6 NaH_2PO_4, 26 $NaHCO_3$, 2 $MgSO_4$, 2 $CaCl_2$, 10 HEPES, and 10 glucose, adjusted to pH 7.4 with NaOH. All experiments were performed at room temperature and completed within 4 to 5 hours of obtaining the brain slice to ensure cell viability. Slices were continuously perfused with aerated aCSF using a gravity-fed perfusion system with a flow rate of 2 to 3 mL/min for the duration of the recording.

Electrophysiology recordings

Whole-cell current-clamp recordings were made from the soma of GnRH-GFP and ARH Kiss1-Cre-GFP neurons. Neurons were identified using a Carl Zeiss Axioskop 2 FS (Jena, Germany) fitted with epifluorescence and infrared-differential contrast video upright microscopy. Patch pipettes were pulled from borosilicate glass capillaries with inner filaments (World Precision Instruments, Sarasota, Florida) using a pp-830 electrode puller (Narishige Scientific Lab Instrument, Tokyo, Japan) and had resistances of 2 to 4 MΩ when filled with a internal pipette solution (in mM): 125 Kgluconate, 2 KCl, 5 MgATP, 0.3 NaGTP, 10 EGTA, and 5 HEPES, adjusted to pH 7.4 with NaOH. Electrophysiological experiments were performed using an Axopatch 200B amplifier, and signals were digitized with Digidata 1322A (Molecular Devices) interfaced to a PC computer. Data were collected using pCLAMP10 software (Molecular Devices) at a sample frequency of 20 kHz, with lowpass filtering at 2 kHz. Whole-cell capacitance and resistance were electronically compensated. Adequate whole-cell access resis-

tance (< 20 MΩ) and membrane resistance (>500 MΩ) were verified at the beginning and the end of the recording. The effects on GnRH neurons were determined by analysis of spontaneous action potential firing and membrane potential change in current-clamp conditions. CART 55–102 was purchased from American Peptide Company (Sunnyvale, California).

Statistics and analysis

Comparisons of cell numbers and mRNA mean integrated intensity were performed by a Student *t* test. Electrophysiological recordings were analyzed with Clampfit-10 software (Molecular Devices). All membrane potentials were corrected by −5 mV for liquid junction potential in final analysis. Statistical evaluation of mean differences in membrane potential after different treatments was performed by one-way ANOVA, with a significance at $P = .05$. Paired *t* test was used to compare action potential firing percentage of GnRH and ARH Kiss1 neurons between control and treatment duration, and *P* value was set at .05 for significance. GraphPad Prism 5 software (GraphPad Software, La Jolla, California) was used for these analyses. All data are expressed as means ± SEM. For event analysis of action potential firing under current clamp conditions, Mini Analysis software (Synaptosoft Inc, Fort Lee, New Jersey) was used. The cells were allowed to stabilize for a minimum of 5 minutes before CART treatment. Recordings were analyzed 3 to 4 minutes before CART application and were used to estimate baseline firing. The change in firing rate after CART was assessed beginning at 5 minutes after CART application as all cells had reached a stable plateau by this time. To quantify the frequency of number of events before and after the application of CART, the calculated events were divided by bin size (60 s).

Results

Experiment 1. Morphological interactions between CART, Kiss1, and GnRH neurons

Immunohistochemistry confirmed that CART fibers are in close apposition with approximately 60% of GnRH neurons (10 cells/animal across 2 sections, n = 6 animals) in the POA (Figure 1). CART fibers in the POA could originate from numerous sources in the hypothalamus or outside areas; however, one population has a unique marker, the ARH CART population coexpresses pro-opiomelanocortin (POMC). Therefore, triple-label immunohistochemistry was used to determine if CART fibers making close appositions to GnRH neurons coexpressed α-MSH, a cleavage product of POMC, indicating an ARH origin. Coexpressing CART/α-MSH fibers make close appositions onto 50% of GnRH cells found in sections just preceding the beginning of the AVPV and to the level of the most rostral AVPV sections (Figure 1). This suggests the vast majority of CART fibers contacting GnRH cells (>80%) likely originate in the ARH.

Double label immunohistochemistry for CART and Kiss1 was undertaken to determine if CART fibers are also in contact with Kiss1 cells. CART-ir fibers were observed to make close appositions to 40% of AVPV Kiss1 cells (an average of 20 cells per animals across 2 sections, n = 6). In the ARH a similar analysis demonstrated that roughly 65% of Kiss1 cells (an average of 40 cells/animal across 3 sections, n = 7 animals) have close appositions from CART fibers. Triple-label immunohistochemistry revealed that a large proportion of CART fibers contacting AVPV and ARH Kiss1 cells coexpress α-MSH, with 30% of AVPV Kiss1 cells having close appositions from CART/α-MSH fibers, whereas 55% of ARH Kiss1 cells had similar close appositions (Figure 1). In the triple-label conditions, single-labeled CART-ir fibers of unknown origin were also found to make close appositions to Kiss1-ir cells, although this was infrequent compared to double-labeled CART/α-MSH-ir contacts (approximately 85%).

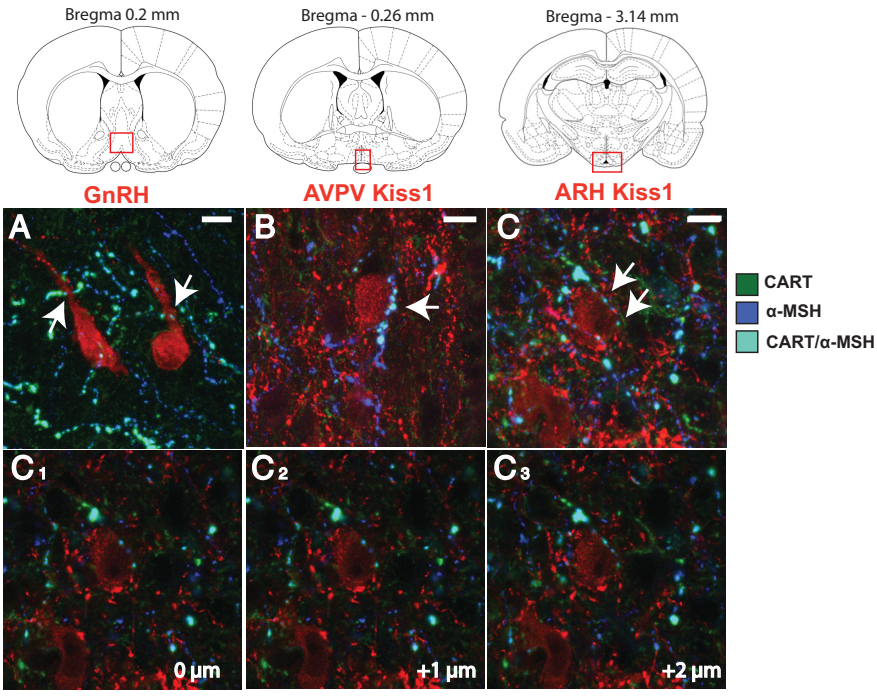

Figure 1. CART close appositions onto GnRH cells in the preoptic area and AVPV and ARH Kiss1 cells. Coexpressing CART/α-MSH-ir (*cyan*) fibers were found in close apposition (*white arrows*) to preoptic area GnRH-GFP cells (A, *pseudocolored red*) as well as AVPV Kiss1-ir cells (B, *red*) and ARH Kiss1-ir cells (C, *red*). Corresponding brain regions where photomicrographs were taken are illustrated. C_1–C_3, single optical slice analysis at 1-μM focal planes illustrating the close apposition of the CART fiber to the ARH Kiss1 cell shown in (C). 10 μM scale bars are given.

Experiment 2. Characterization of CART effects on GnRH cell firing

CART application to GnRH-GFP neurons resulted in activation of firing and depolarization under whole-cell current-clamp conditions (Figure 2A). Twelve of 16 (75%) of the GnRH cells tested responded to CART, in general agreement with the estimate of CART fiber contacts onto GnRH cells (Figure 1). CART (100 nM) application significantly increased firing frequency from a basal firing frequency of 1.1 ± 0.6 Hz to 3.5 ± 1.4 Hz after CART administration and the effect persisted long after washout with this maximum concentration of the drug (n = 8 cells, *t* test, $P < .05$, Figure 2B). CART application also resulted in a significant membrane depolarization of 11.04 ± 2 mV, from an average resting membrane potential of −60.43 ± 0.8 mV to −49.4 ± 1.4 mV post-CART (n = 12 cells, *t* test, $P < .0001$).

To establish whether CART-induced stimulation was presynaptic or postsynaptic, the effects of CART on GnRH neurons were tested after pre-exposure to tetrodotoxin (TTX, 1 μM), to block voltage-gated sodium channels. Roughly 80% of cells responded to various concentrations of CART (1, 3, 10, 30, 100, and 300 nM). Only one cell was recorded from each slice, and typically one and a maximum of 3 concentrations were tested on the cells that were able to recover completely after wash-off (n = 39, with minimum of 5 cells for each concentration). With 100 nM CART under TTX, it took an average of 9.1 ± 0.7 minutes from the time of CART application to reach peak depolarization, and the cells did not fully recover to baseline membrane potential for the duration of the recording (Figure 2C). The estimated EC_{50} for CART-induced depolarization was 37.4 ± 1.6 nM (Figure 2D). CART (100 nM) evoked a maximum depolarization of 13 ± 1.4 mV; this was similar to the depolarization observed in the absence of TTX (11.04 ± 2 mV, Figure 2A), suggesting that CART's ability to stimulate free-firing GnRH neurons is predominantly due to direct postsynaptic activation.

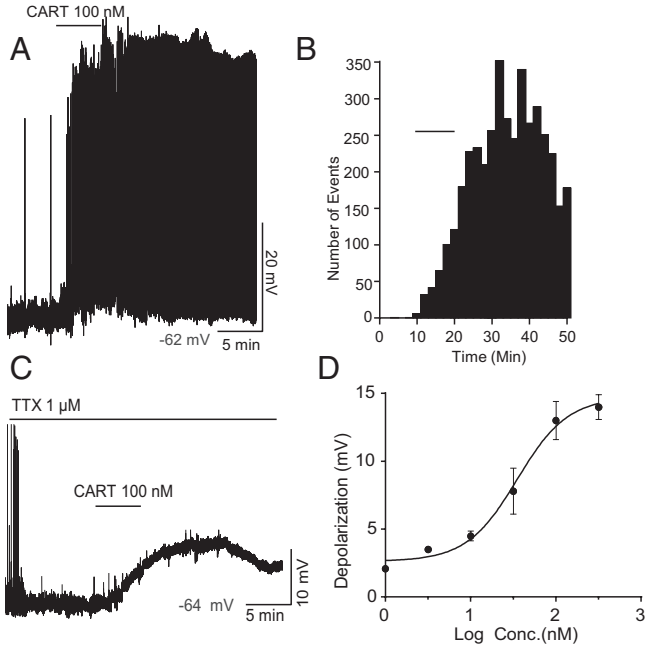

Figure 2. CART activates GnRH-GFP neurons. (A) A representative current clamp recording showing 100 nM CART-induced depolarization and spontaneous firing in GnRH-GFP neurons. The resting membrane potential was −62 mV. (B) Histogram for the representative recording shown in (A) showing firing increased from 0.34 to 4.28 events per minute. (C) A representative current-clamp recording under TTX showing 100 nM CART induced a maximum depolarization of 13 ± 1.4 mV. The resting membrane potential was −64 mV. (D) Concentration versus response curve for the CART induced depolarization of GnRH neurons. EC_{50} = 37.4 ± 1.6 nM. Data are presented as mean ± SEM. N = 39 cells, with 10 nonresponders (n = 5, 5, 6, 6, 11, and 6 cells for 1, 3, 10, 30, 100, and 300 nM CART, respectively).

Experiment 3. Characterization of CART effects on ARH Kiss1 cell firing

Evidence of CART fibers in close contact with Kiss1 cells led to the hypothesis that CART may also be capable of regulating Kiss1 cell firing. Whole-cell current-clamp recordings from slices taken from OVX Kiss1-Cre-GFP mice revealed that ARH Kiss1 neurons exhibit spontaneous action potential firing similar to GnRH neurons. CART (30 nM) application increased the action potential firing from 0.67 ± 0.25 Hz to 2.12 ± 0.73 Hz (n = 5 cells, *t* test, $P < .05$; Figure 3A); this effect was long-lasting and persisted long after drug washout (Figure 3B), similar to its effect on GnRH. CART depolarized Kiss1 neurons by 13.6 mV, from a resting membrane potential of −69.1 ± 3.8 mV to −55.5 ± 2.9 mV post-CART treatment (n = 5 cells, paired *t* test, $P < .05$). This depolarization in response to 30 nM CART was equivalent to the depolarization caused by 100 nM CART on GnRH cells (Figure 2).

To determine whether CART effects on Kiss1 cell firing were pre- or postsynaptic, 30 nM CART application was investigated in the presence of TTX. CART application resulted in a significant depolarization of ARH Kiss1 cells in the presence of TTX; it took an average of 10 ± 1.6 minutes from the time of CART application to reach peak depolarization, and the cells did not fully recover to baseline membrane potential for the duration of the recording (Figure 3C). Under TTX conditions, 30 nM CART depolarized Kiss1 neurons by 13.5 mV, from an average resting membrane potential of −62.2 ± 5.06 mV to −48.7 ± 3.4 mV (n = 10 cells, *t* test, $P < .005$; Figure 3D). The similar degree of depolarization in response to CART in the absence or presence of TTX indicates CART's effects on Kiss1 cells are primarily due to direct postsynaptic actions. In comparing the effects of 30 nM CART under TTX on

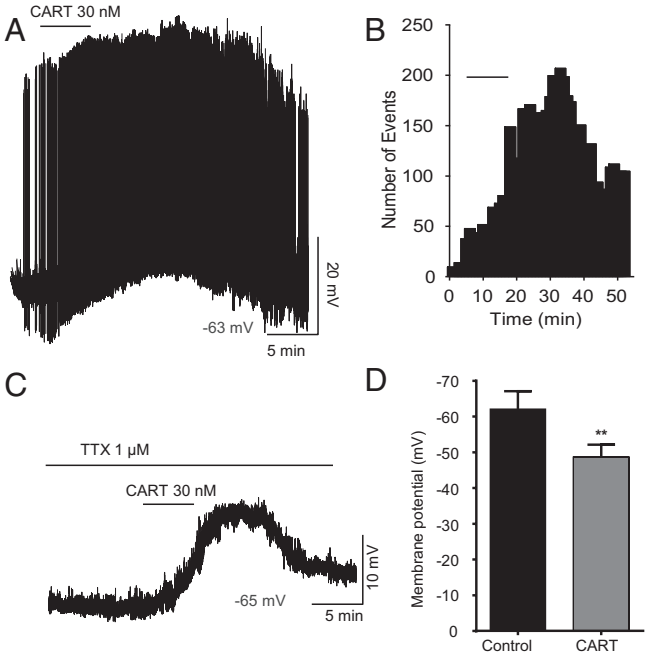

Figure 3. CART depolarizes Kiss1-GFP neurons in the mouse. (A) A representative current-clamp recording showing spontaneous firing in Kiss1 neurons and CART induced depolarization under no presynaptic input block condition. The resting membrane potential was −63 mV. (B) Histogram for the representative recording shown in (A) showing firing increased from 1.4 to 3.64 events per minute. (C) A representative current-clamp recording under TTX showing 30 nM CART induced depolarization. The resting membrane potential was −65 mV. (D) Summary of the significant depolarizing effect of CART in the presence of TTX (control, −62.2 ± 5.06 mV; CART, −48.7 ± 3.4 mV; $P < .005$).

Kiss1 and GnRH cells, the 13.5-mV depolarization of Kiss1 cells compares with 7.3-mV depolarization of GnRH cells (Figure 2D; n = 6 cells), indicating that Kiss1 cells may be more sensitive to the effects of CART. However, all other aspects, such as the onset of the response to CART, and the very prolonged duration of the response, particularly to maximum doses of CART, were similar between Kiss1 and GnRH cells.

Experiment 4. Differential regulation of CART populations during negative energy balance

Caloric restriction

CART protein and mRNA levels were examined by immunohistochemistry and in situ hybridization, respectively, in the ARH and AVPV following a 12-day 50% CR. The number of CART-ir cells in the ARH CART-ir was significantly lower in CR animals compared to ad libitum fed controls (cell count: ad libitum 218 ± 19, CR 139.5 ± 9, *t* test, $P = .004$; Figure 4A). ARH CART mRNA levels were also significantly decreased in CR animals (mean integrated intensity: ad libitum 11 932 ± 2342, CR 2527 ± 454, *t* test, $P < .005$; Figure 4B). In contrast, AVPV CART-ir cell numbers were not significantly different between ad libitum fed and CR animals (cell count: ad libitum 17.6 ± 2, CR 15.3 ± 2, *t* test, $P = .45$); however, the few number of cells that could be identified in this area by immunohistochemistry would likely make it difficult to detect significant differences between the 2 groups (Figure 5A). In situ hybridization demonstrated that AVPV CART mRNA was significantly lower in CR animals compared to ad libitum fed controls (mean integrated intensity: ad libitum 1262 ± 285, CR 281 ± 150, *t* test, $P = .04$; Figure 5B). In the DMH, there was no significant difference in the number of CART-ir cells between ad libitum fed and CR animals (cell count: ad libitum 9 ± 1.8, CR 13 ± 1.8, *t* test, $P = .15$) or in CART mRNA levels (integrated intensity: ad libitum 3791 ± 1034, CR 1722 ± 308, *t* test, $P = .08$) (Supplemental Figure 1, published on The Endocrine Society's Journals Online web site at http://jcem.endojournals.org).

Lactation

The number of ARH CART-ir cells was not significantly different between controls and lactating animals (cell count: virgin 151.7 ± 9.6, lactation 130.3 ± 4.1, *t* test, $P = .08$; Figure 6A). Similarly, in situ hybridization demonstrated no significant difference in CART mRNA levels during lactation in the ARH (mean integrated intensity: virgin 6439 ± 1707, lactation 5044 ± 1357, *t* test, $P = .55$; Figure 6B). AVPV CART-ir cell numbers revealed a dramatic greater than 3-fold increase in the number of CART cells during lactation (cell count: virgin 43.5 ± 6, lactation 145.3 ± 18.8, *t* test, $P < .001$; Figure 7A). This increase in CART protein accumulation in the cell body was accompanied by a small insignificant decrease in AVPV CART mRNA levels during lactation (mean integrated intensity: virgin 672.6 ± 168, lactation 381.2 ± 80, *t* test, $P = .17$; Figure 7B). DMH CART protein (cell count: virgin 7 ± 3.2, lactation 5.7 ± 1.3, *t* test, $P = .72$) and mRNA levels (integrated intensity: virgin 1243 ± 318, lactation 3210 ± 949, *t* test, $P = .06$) were not significantly altered during lactation (Supplemental Figure 2).

The increase in AVPV CART-ir cells was similar to our previously reported findings of increased AVPV Kiss1-ir cells during lactation (14). Thus, double-label immunohistochemistry was performed to determine if the 2 neuropeptides were coexpressed in the same cells of the AVPV. Notably AVPV CART-ir and Kiss1-ir showed no colocalization of cell bodies during lactation (Supplemental Figure 3) or control conditions (data not shown). CART-ir cells were most abundant in the most rostral sections of the AVPV, whereas Kiss1-ir cells were concentrated in the more caudal sections of the periventricular region (Supplemental Figure 3).

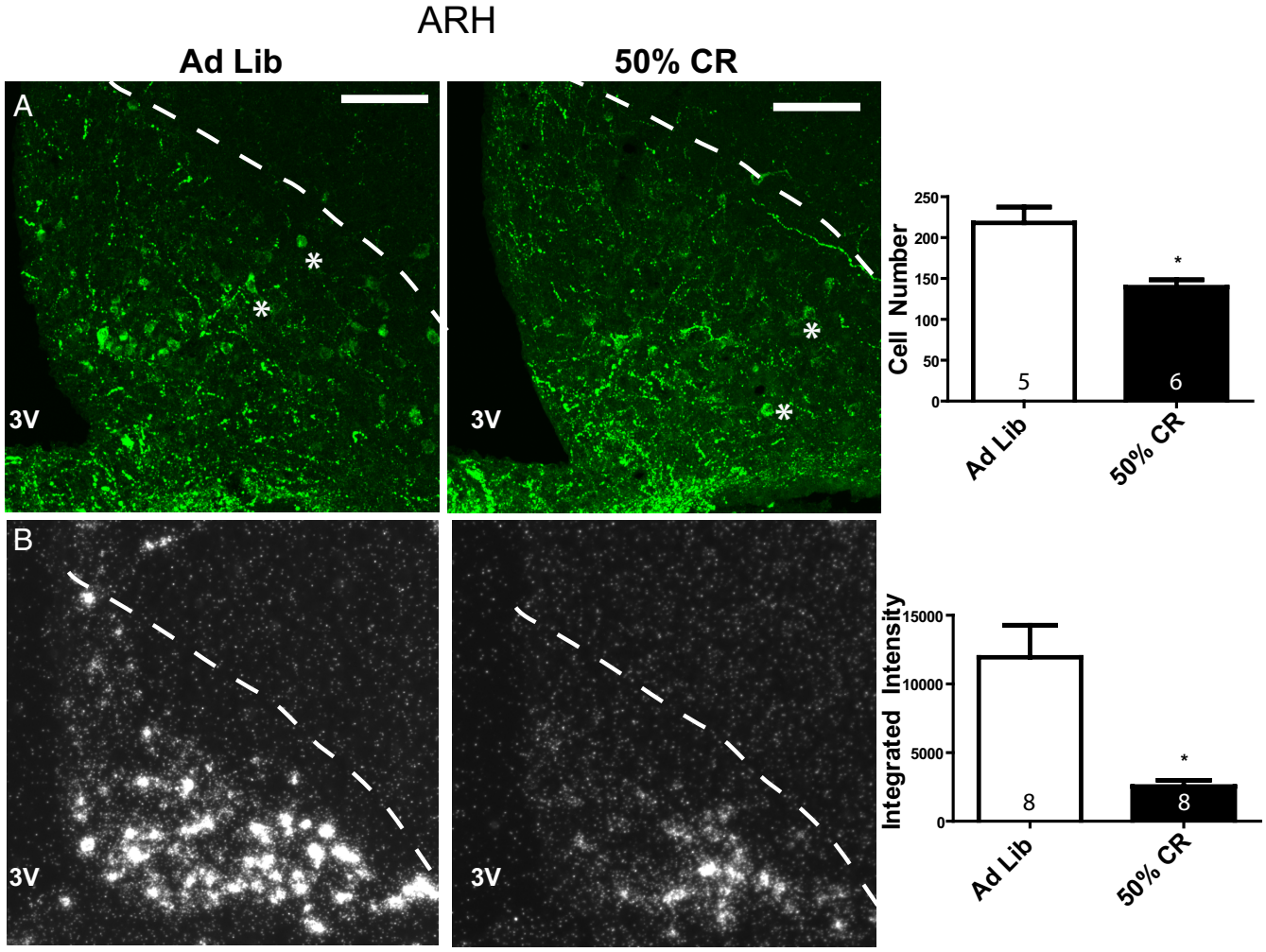

Figure 4. Arcuate nucleus CART protein and mRNA levels during CR. (A) Confocal photomicrographs of immunohistochemistry for CART protein (Phoenix antibody, H-003–62) in the ARH (location denoted by dotted line) in ad libitum fed and 50% CR animals (100 μM scale bar provided). Quantification of the total number ARH CART cells in 4 sections per animal is provided in the bar graph. (B) Dark field silver grain photomicrographs of in situ hybridization for ^{35}S-CART mRNA probe. Quantification of ARH CART mRNA mean integrated intensities is provided in the histogram. Group sample size is given within each histogram. 3V, third ventricle. *, examples of identified cells.

Discussion

This study provides compelling evidence for a novel role of CART in the regulation of the reproductive neuroendocrine axis. CART's ability to stimulate firing in both ARH Kiss1 and GnRH cells directly demonstrates that CART may regulate GnRH release both directly and indirectly. Given CART's known role in energy homeostasis, we hypothesize that CART may provide an important link between reproductive and metabolic hypothalamic circuits. Consistent with this hypothesis, ARH and AVPV CART mRNA levels are inhibited during CR; therefore, inhibition of stimulatory CART expression could contribute to inhibition of to Kiss1 and GnRH release during negative metabolic states. Electrophysiological experiments examining whether CART tone on Kiss1 and GnRH neurons is altered during CR will be an important next step to determine the causative role of decreased CART expression in the inhibition of reproductive function.

Although previous experiments have examined the morphological relationship between CART and GnRH cells, only one recent study (38) has examined CART's effects on GnRH cell firing. CART stimulated GnRH neuronal firing in mice; however, the percentage of GnRH cells that were sensitive to CART was reportedly much lower than the findings presented here in the rat. A possible explanation for this discrepancy is that the previous study tested only a few numbers of cells, possibly leading to an underestimation of the number of CART-responsive GnRH cells. Most GnRH neurons also respond robustly to CART administration under TTX conditions, indicating for the first time a direct postsynaptic effect of CART on GnRH neurons. This result is consistent with the observation of CART fibers in close contact with most

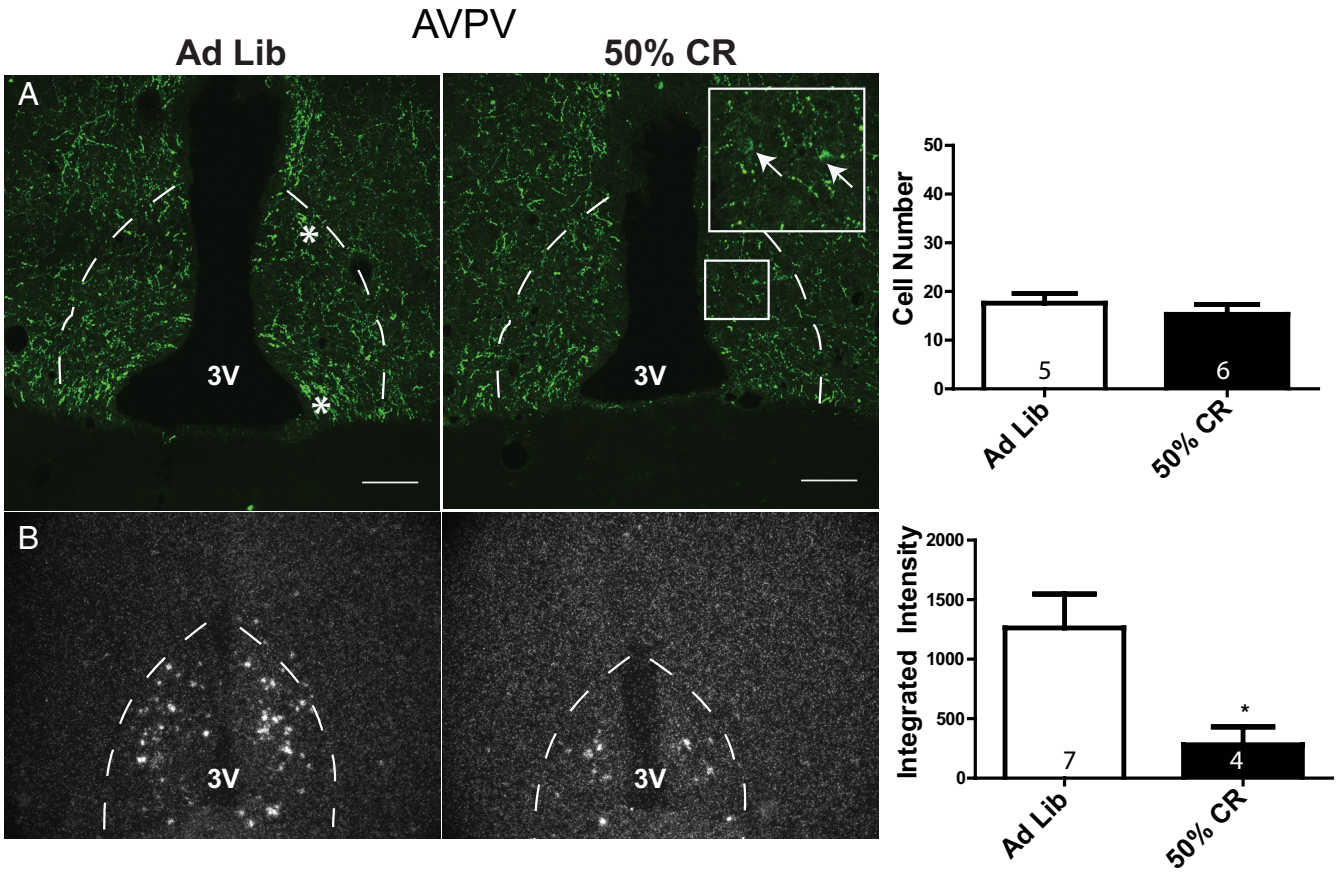

Figure 5. Anteroventral periventricular nucleus CART protein and mRNA levels during CR. (A) Confocal photomicrographs of immunohistochemistry for CART protein in the AVPV (location denoted by dotted line) in ad libitum fed and 50% CR animals (100 μM scale bar provided). Quantification of the total number of AVPV CART cells observed in 3 sections per animal is provided in the bar graph. (B) Dark field silver grain photomicrographs of in situ hybridization for ^{35}S-CART mRNA probe. Quantification of AVPV CART mRNA mean integrated intensities is provided in the histogram. Group sample size is given within each histogram. 3V, third ventricle. *, examples of identified cells.

GnRH neurons noted here and in previous studies (10, 11). Further highlighting an important role of CART in reproductive regulation is the finding that CART directly stimulates ARH Kiss1 cells, confirming neuroanatomical data showing CART fibers in close contact with the ARH Kiss1 population. Thus, CART has similar excitatory actions on GnRH and Kiss1 cells that are postsynaptic in nature.

Many other appetitive neuropeptides have been linked to the regulation of GnRH release, and CART should now be included among these known regulators of both metabolic and reproductive circuits (11, 39–44). However, CART is the first appetitive neuropeptide to our knowledge capable of also regulating Kiss1 release. Therefore, CART regulates GnRH neurons at 2 levels of the reproductive circuitry, through Kiss1 neurons that project to GnRH cell bodies (14) and through direct actions on GnRH cells, pointing to a possible increased regulatory influence over the Kiss1/GnRH system compared to other metabolic neuropeptides. Interestingly, the CART receptors have yet to be identified; therefore, more detailed electrophysiological studies will aid in determining the types of channels activated by CART administration, whether they can account for the apparent greater sensitivity of ARH Kiss1 than GnRH cells to CART, and if there are species differences in responses to CART.

Previous neuronal tract tracing studies have provided evidence that CART cells in the ARH, DMH, AVPV, and the ventral premammillary nucleus all send projections to the POA (11), and CART cells are also found in the lateral hypothalamus, another region known to be involved in GnRH regulation (33, 45). These findings highlight the potential for several CART populations to regulate GnRH neurons directly in vivo. Inhibition of CART mRNA levels in the ARH and AVPV during CR may directly result in decreased stimulatory input to GnRH neurons and contribute to anovulation. Importantly, most CART fibers contacting GnRH cells as well as ARH and AVPV Kiss1 cells coexpressed the POMC cleavage product α-MSH. Based on these results, we hypothesize that the ARH CART population is the dominant CART population regulating ARH and AVPV Kiss1 and GnRH neuronal firing.

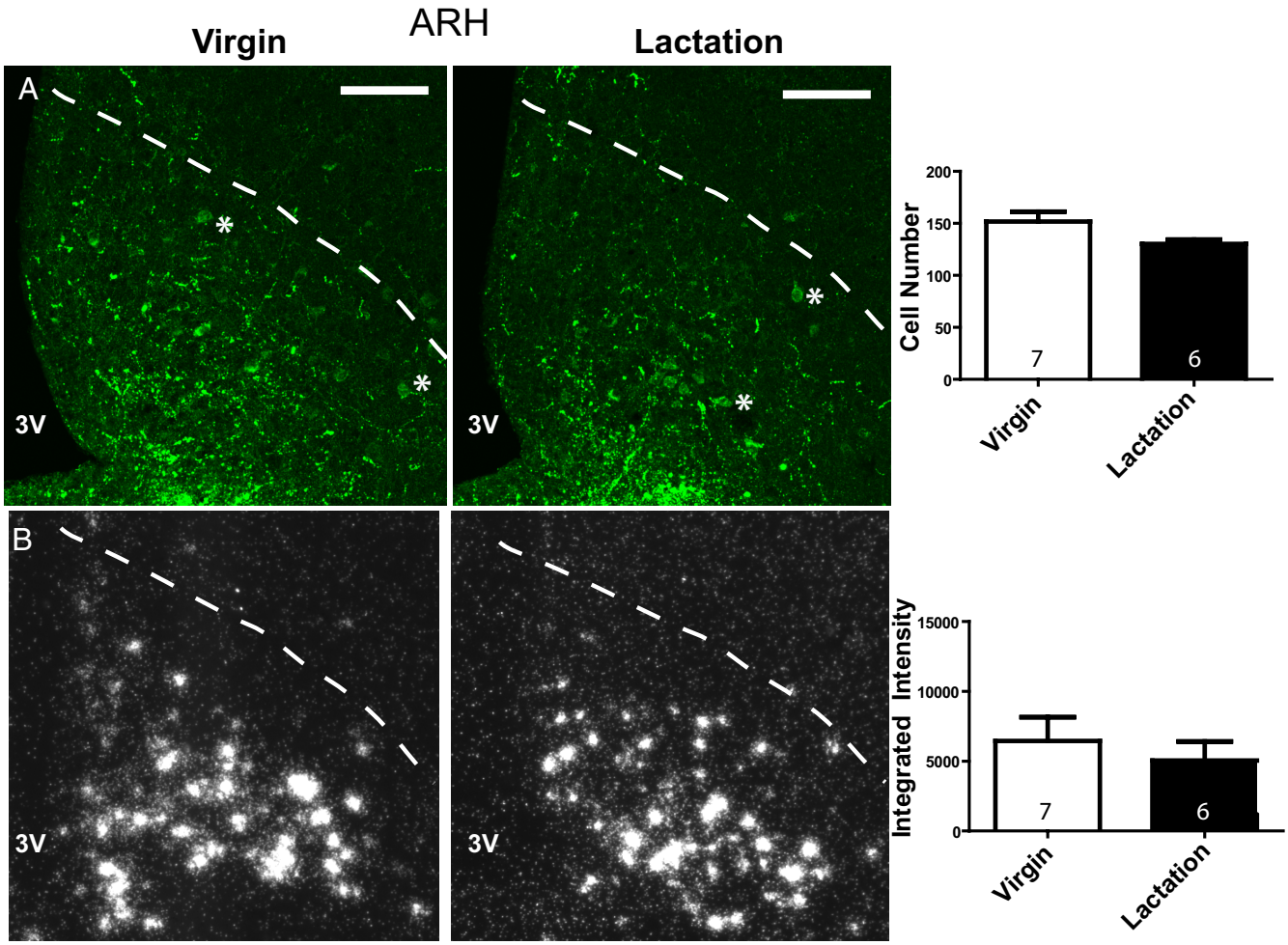

Figure 6. Arcuate nucleus CART protein and mRNA levels during lactation. (A) Confocal photomicrographs of immunohistochemistry for CART protein in the ARH (location denoted by dotted line) during virgin control and lactation conditions (100 μM scale bar provided). Quantification of the total number of ARH CART cells in 4 sections per animal is provided in the bar graph. (B) Dark field silver grain photomicrographs of in situ hybridization for ^{35}S-CART mRNA probe. Quantification of ARH CART mRNA mean integrated intensities is provided in the histogram. Group sample size is given within each histogram. 3V, third ventricle. *, examples of identified cells.

The effects of POMC on ARH Kiss1 neuronal firing have not yet been tested, but α-MSH has been reported to stimulate GnRH neurons (38, 46). Investigations of the interaction of CART and POMC cleavage products, α-MSH and β-endorphin, on Kiss1 and GnRH cells will likely be important for our understanding of the role of these ARH cells in reproductive regulation. Interestingly, Kiss1 excites ARH POMC/CART cells, highlighting the complex degree of interconnectivity likely occurring between reproductive and metabolic hypothalamic neurons (47).

Although CART expression is inhibited during CR, there is surprisingly little regulation of CART during lactation, although only a specific time point of midlactation was investigated, making it possible that CART may be regulated at later stages of lactation. These 2 models both result in negative energy balance but by different mechanisms: undernutrition during CR, and elevated energy expenditure during lactation. One hypothesis is that undernutrition is specifically required for ARH and AVPV CART inhibition, and that lactation-induced hyperphagia prevents this inhibition. Interestingly, POMC is not inhibited during CR when CART levels are decreased, but POMC is inhibited during lactation when CART expression is unaffected (1, 25, 48). This suggests that POMC and CART may be regulated by differential signals and affect distinct downstream changes in both metabolic and reproductive circuits.

Although CART mRNA levels were unaffected during lactation, there was a surprising increase in AVPV CART-ir neurons during this condition. The protein accumulation in AVPV CART cells during lactation is strikingly similar to results observed in AVPV Kiss1 cells during lactation (14). Although AVPV CART mRNA was not significantly decreased during lactation, as has been reported for AVPV Kiss1 mRNA, it is clear that increases in CART mRNA production do not account for increased

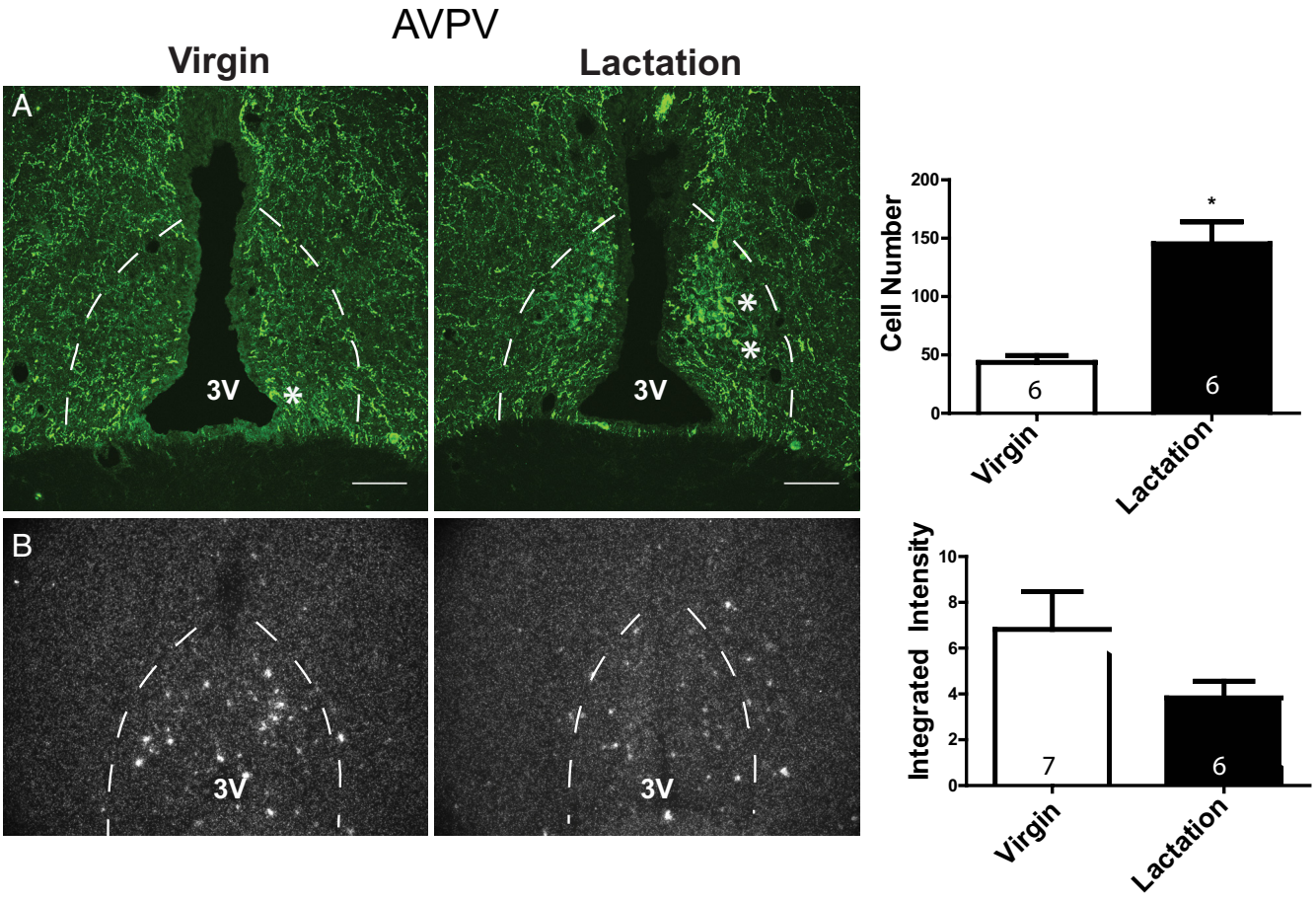

Figure 7. Anteroventral periventricular nucleus CART protein and mRNA levels during lactation. (A) Confocal photomicrographs of immunohistochemistry for CART protein in the AVPV (location denoted by dotted line) during virgin control and lactation conditions (100 μM scale bar provided). Quantification of the total number of AVPV CART cells in 3 sections per animal is provided in the bar graph. (B) Dark field silver grain photomicrographs of in situ hybridization for ^{35}S-CART mRNA probe. Quantification of AVPV CART mRNA mean integrated intensities is provided in the histogram. Group sample size is given within each histogram. 3V, third ventricle. *, examples of identified cells.

protein levels. Interpretation of opposing changes in protein and mRNA levels in the AVPV is difficult and could lead to 2 different hypotheses. One is that like AVPV Kiss1 cells, AVPV CART cells have inhibited protein release during lactation, leading to accumulation of protein in cell bodies. Another is that there is an increase in CART translation leading to an increase in secretion. Therefore, at this time the role of the AVPV CART population during lactation remains unclear. This is in contrast to CR in which CART cells in the AVPV and ARH are both clearly inhibited.

Consistently we find a striking similarity between CART and Kiss1 systems. There are significant populations of both neuropeptides in the AVPV and ARH, 2 nuclei with known roles in reproductive function (29, 49, 50). CART and Kiss1 populations in the ARH and AVPV appear inhibited during negative energy balance (1, 8, 14), and both ARH CART and Kiss1 populations, as well as AVPV Kiss1 cells, appear in direct contact with GnRH cells (14). Kiss1 is a well-known and extremely potent stimulator of GnRH firing (51), and the current study provides evidence that CART also strongly stimulates GnRH neurons. The maximum depolarization achieved by CART (100 nM, 13 ± 1.4 mV, under TTX conditions) is only about 7 mV less than that achieved by Kiss1 (Kp-10 agonist, 100 nM, 20.2 ± 1.2 mV, under TTX conditions) (Verma, S., K. L. Grove, and M. S. Smith, unpublished data). It is also interesting to note that the long duration of the response to CART on both GnRH and Kiss1 cells is very similar in nature to the long duration of the stimulatory effects of Kiss1 on GnRH cells (52). These similarities highlight an emerging understanding of the importance for CART in reproductive regulation.

Beyond CART's role in negative energy balance, it is possible that CART also plays a role in tonic pulsatile and surge mechanisms of GnRH release through the estrous cycle given 1) previous evidence that ARH CART/POMC cells have augmented burst firing in response to estrogen (53, 54) and 2) the observed connections between CART cells and ARH and AVPV Kiss1 populations, which are

known to contribute to positive and negative feedback effects of estrogen on GnRH neurons (24, 50, 55). CART fibers are observed in close apposition with GnRH neurons expressing c-Fos on the afternoon of proestrus (11); thus, it is possible that ARH CART cells may be stimulated by increased estrogen levels leading not only to activation of AVPV Kiss1 cells, which are known to contribute to the proestrous GnRH surge, but also to direct activation of GnRH neurons. Additionally, CART may contribute to the regulation of basal, pulsatile GnRH release through activation of both ARH Kiss1 cells and GnRH cells directly. Overall, the current findings point to a significant and newly defined role for CART in the regulation of reproductive circuits. Understanding the upstream regulators and downstream effectors of hypothalamic CART neurons will be an important next step toward understanding the mechanisms of association and interregulation of hypothalamic reproductive and metabolic circuits.

Acknowledgments

The authors acknowledge the National Institutes of Health grants that supported this work (HD014643, P51 OD011092), the Oregon National Primate Research Center Imaging and Morphology Support Core, and Dr Anda Cornea for assistance with confocal microscopy.

Address all correspondence and requests for reprints to: Dr M. Susan Smith, 505 NW 185th Avenue, Beaverton, OR 97006. E-mail: smithsu@ohsu.edu.

Disclosure Summary: The authors declare no competing financial interests.

References

1. **True C, Kirigiti MA, Kievit P, Grove KL, Smith MS.** Leptin is not the critical signal for kisspeptin or luteinising hormone restoration during exit from negative energy balance. *J Neuroendocrinol*. 2011;23:1099–1112.
2. **Ahima RS, Prabakaran D, Mantzoros C, et al.** Role of leptin in the neuroendocrine response to fasting. *Nature*. 1996;382:250–252.
3. **Szymanski LA, Schneider JE, Friedman MI, et al.** Changes in insulin, glucose and ketone bodies, but not leptin or body fat content precede restoration of luteinising hormone secretion in ewes. *J Neuroendocrinol*. 2007;19:449–460.
4. **Welt CK, Chan JL, Bullen J, et al.** Recombinant human leptin in women with hypothalamic amenorrhea. *N Engl J Med*. 2004;351:987–997.
5. **Smith MS, True C, Grove KL.** The neuroendocrine basis of lactation-induced suppression of GnRH: role of kisspeptin and leptin. *Brain Res*. 2010;1364:139–152.
6. **Kong W, Stanley S, Gardiner J, et al.** A role for arcuate cocaine and amphetamine-regulated transcript in hyperphagia, thermogenesis, and cold adaptation. *FASEB J*. 2003;17:1688–1690.
7. **Elias CF, Lee C, Kelly J, et al.** Leptin activates hypothalamic CART neurons projecting to the spinal cord. *Neuron*. 1998;21:1375–1385.
8. **Kristensen P, Judge ME, Thim L, et al.** Hypothalamic CART is a new anorectic peptide regulated by leptin. *Nature*. 1998;393:72–76.
9. **Abbott CR, Rossi M, Wren AM, et al.** Evidence of an orexigenic role for cocaine- and amphetamine-regulated transcript after administration into discrete hypothalamic nuclei. *Endocrinology*. 2001;142:3457–3463.
10. **Leslie RA, Sanders SJ, Anderson SI, Schuhler S, Horan TL, Ebling FJ.** Appositions between cocaine and amphetamine-related transcript- and gonadotropin releasing hormone-immunoreactive neurons in the hypothalamus of the Siberian hamster. *Neurosci Lett*. 2001;314:111–114.
11. **Rondini TA, Baddini SP, Sousa LF, Bittencourt JC, Elias CF.** Hypothalamic cocaine- and amphetamine-regulated transcript neurons project to areas expressing gonadotropin releasing hormone immunoreactivity and to the anteroventral periventricular nucleus in male and female rats. *Neuroscience*. 2004;125:735–748.
12. **Robson AJ, Rousseau K, Loudon AS, Ebling FJ.** Cocaine and amphetamine-regulated transcript mRNA regulation in the hypothalamus in lean and obese rodents. *J Neuroendocrinol*. 2002;14:697–709.
13. **Adam CL, Archer ZA, Findlay PA, Thomas L, Marie M.** Hypothalamic gene expression in sheep for cocaine- and amphetamine-regulated transcript, pro-opiomelanocortin, neuropeptide Y, agouti-related peptide and leptin receptor and responses to negative energy balance. *Neuroendocrinology*. 2002;75:250–256.
14. **True C, Kirigiti M, Ciofi P, Grove KL, Smith MS.** Characterisation of arcuate nucleus kisspeptin/neurokinin B neuronal projections and regulation during lactation in the rat. *J Neuroendocrinol*. 2011;23:52–64.
15. **Castellano JM, Navarro VM, Fernández-Fernández R, et al.** Changes in hypothalamic KiSS-1 system and restoration of pubertal activation of the reproductive axis by kisspeptin in undernutrition. *Endocrinology*. 2005;146:3917–3925.
16. **Castellano JM, Navarro VM, Fernández-Fernández R, et al.** Expression of hypothalamic KiSS-1 system and rescue of defective gonadotropic responses by kisspeptin in streptozotocin-induced diabetic male rats. *Diabetes*. 2006;55:2602–2610.
17. **Forbes S, Li XF, Kinsey-Jones J, O'Byrne K.** Effects of ghrelin on Kisspeptin mRNA expression in the hypothalamic medial preoptic area and pulsatile luteinising hormone secretion in the female rat. *Neurosci Lett*. 2009;460:143–147.
18. **Kalamatianos T, Grimshaw SE, Poorun R, Hahn JD, Coen CW.** Fasting reduces KiSS-1 expression in the anteroventral periventricular nucleus (AVPV): effects of fasting on the expression of KiSS-1 and neuropeptide Y in the AVPV or arcuate nucleus of female rats. *J Neuroendocrinol*. 2008;20:1089–1097.
19. **Backholer K, Smith JT, Rao A, et al.** Kisspeptin cells in the ewe brain respond to leptin and communicate with neuropeptide Y and pro-opiomelanocortin cells. *Endocrinology*. 2010;151:2233–2243.
20. **Wahab F, Ullah F, Chan YM, Seminara SB, Shahab M.** Decrease in hypothalamic Kiss1 and Kiss1r expression: a potential mechanism for fasting-induced suppression of the HPG axis in the adult male rhesus monkey (Macaca mulatta). *Horm Metab Res*. 2011;43:81–85.
21. **Xu J, Kirigiti MA, Cowley MA, Grove KL, Smith MS.** Suppression of basal spontaneous gonadotropin-releasing hormone neuronal activity during lactation: role of inhibitory effects of neuropeptide Y. *Endocrinology*. 2009;150:333–340.
22. **Goodman RL.** A quantitative analysis of the physiological role of estradiol and progesterone in the control of tonic and surge secretion of luteinizing hormone in the rat. *Endocrinology*. 1978;102:142–150.
23. **Gottsch ML, Popa SM, Lawhorn JK, et al.** Molecular properties of Kiss1 neurons in the arcuate nucleus of the mouse. *Endocrinology*. 2011;152:4298–4309.
24. **Smith JT, Cunningham MJ, Rissman EF, Clifton DK, Steiner RA.**

Regulation of Kiss1 gene expression in the brain of the female mouse. *Endocrinology*. 2005;146:3686–3692.
25. **Xu J, Kirigiti MA, Grove KL, Smith MS.** Regulation of food intake and gonadotropin-releasing hormone/luteinizing hormone during lactation: role of insulin and leptin. *Endocrinology*. 2009;150:4231–4240.
26. **Elias CF, Saper CB, Maratos-Flier E, et al.** Chemically defined projections linking the mediobasal hypothalamus and the lateral hypothalamic area. *J Comp Neurol*. 1998;402:442–459.
27. **Franceschini I, Lomet D, Cateau M, Delsol G, Tillet Y, Caraty A.** Kisspeptin immunoreactive cells of the ovine preoptic area and arcuate nucleus co-express estrogen receptor alpha. *Neurosci Lett*. 2006;401:225–230.
28. **Kirouac GJ, Parsons MP, Li S.** Innervation of the paraventricular nucleus of the thalamus from cocaine- and amphetamine-regulated transcript (CART) containing neurons of the hypothalamus. *J Comp Neurol*. 2006;497:155–165.
29. **Gottsch ML, Cunningham MJ, Smith JT, et al.** A role for kisspeptins in the regulation of gonadotropin secretion in the mouse. *Endocrinology*. 2004;145:4073–4077.
30. **Gee CE, Chen CL, Roberts JL, Thompson R, Watson SJ.** Identification of proopiomelanocortin neurones in rat hypothalamus by in situ cDNA-mRNA hybridization. *Nature*. 1983;306:374–376.
31. **Hoffman GE, Le WW, Sita LV.** The importance of titrating antibodies for immunocytochemical methods. *Curr Protoc Neurosci*. 2008;Chapter 2: Unit 2.12.
32. **Elias CF, Lee CE, Kelly JF, et al.** Characterization of CART neurons in the rat and human hypothalamus. *J Comp Neurol*. 2001;432:1–19.
33. **Vrang N, Larsen PJ, Clausen JT, Kristensen P.** Neurochemical characterization of hypothalamic cocaine- amphetamine-regulated transcript neurons. *J Neurosci*. 1999;19:RC5.
34. **Brailoiu GC, Dun SL, Ohsawa M, et al.** KiSS-1 expression and metastin-like immunoreactivity in the rat brain. *J Comp Neurol*. 2005;481:314–329.
35. **Li C, Chen P, Smith MS.** Morphological evidence for direct interaction between arcuate nucleus neuropeptide Y (NPY) neurons and gonadotropin-releasing hormone neurons and the possible involvement of NPY Y1 receptors. *Endocrinology*. 1999;140:5382–5390.
36. **Campbell RE, Grove KL, Smith MS.** Gonadotropin-releasing hormone neurons coexpress orexin 1 receptor immunoreactivity and receive direct contacts by orexin fibers. *Endocrinology*. 2003;144:1542–1548.
37. **Lee SJ, Kirigiti M, Lindsley SR, et al.** Efferent projections of neuropeptide Y-expressing neurons of the dorsomedial hypothalamus in chronic hyperphagic models. *J Comp Neurol*. 2013;521:1891–1914.
38. **Roa J, Herbison AE.** Direct regulation of GnRH neuron excitability by arcuate nucleus POMC and NPY neuron neuropeptides in female mice. *Endocrinology*. 2012;153:5587–5599.
39. **Lebrethon MC, Aganina A, Fournier M, Gérard A, Parent AS, Bourguignon JP.** Effects of in vivo and in vitro administration of ghrelin, leptin and neuropeptide mediators on pulsatile gonadotrophin-releasing hormone secretion from male rat hypothalamus before and after puberty. *J Neuroendocrinol*. 2007;19:181–188.
40. **Bohler HC Jr, Tracer H, Merriam GR, Petersen SL.** Changes in proopiomelanocortin messenger ribonucleic acid levels in the rostral periarcuate region of the female rat during the estrous cycle. *Endocrinology*. 1991;128:1265–1269.
41. **Cheung S, Hammer RP Jr.** Gonadal steroid hormone regulation of proopiomelanocortin gene expression in arcuate neurons that innervate the medial preoptic area of the rat. *Neuroendocrinology*. 1995;62:283–292.
42. **Hill JW, Elmquist JK, Elias CF.** Hypothalamic pathways linking energy balance and reproduction. *Am J Physiol Endocrinol Metab*. 2008;294:E827–E832.
43. **Lebrethon MC, Vandersmissen E, Gérard A, Parent AS, Bourguignon JP.** Cocaine and amphetamine-regulated-transcript peptide mediation of leptin stimulatory effect on the rat gonadotropin-releasing hormone pulse generator in vitro. *J Neuroendocrinol*. 2000;12:383–385.
44. **Gaskins GT, Moenter SM.** Orexin a suppresses gonadotropin-releasing hormone (GnRH) neuron activity in the mouse. *Endocrinology*. 2012;153:3850–3860.
45. **Williamson-Hughes PS, Grove KL, Smith MS.** Melanin concentrating hormone (MCH): a novel neural pathway for regulation of GnRH neurons. *Brain Res*. 2005;1041:117–124.
46. **Israel DD, Sheffer-Babila S, de Luca C, et al.** Effects of leptin and melanocortin signaling interactions on pubertal development and reproduction. *Endocrinology*. 2012;153:2408–2419.
47. **Fu LY, van den Pol AN.** Kisspeptin directly excites anorexigenic proopiomelanocortin neurons but inhibits orexigenic neuropeptide Y cells by an indirect synaptic mechanism. *J Neurosci*. 2010;30:10205–10219.
48. **Smith MS.** Lactation alters neuropeptide-Y and proopiomelanocortin gene expression in the arcuate nucleus of the rat. *Endocrinology*. 1993;133:1258–1265.
49. **Smith JT, Dungan HM, Stoll EA, et al.** Differential regulation of KiSS-1 mRNA expression by sex steroids in the brain of the male mouse. *Endocrinology*. 2005;146:2976–2984.
50. **Adachi S, Yamada S, Takatsu Y, et al.** Involvement of anteroventral periventricular metastin/kisspeptin neurons in estrogen positive feedback action on luteinizing hormone release in female rats. *J Reprod Dev*. 2007;53:367–378.
51. **Zhang C, Bosch MA, Rønnekleiv OK, Kelly MJ.** Gamma-aminobutyric acid B receptor mediated inhibition of gonadotropin-releasing hormone neurons is suppressed by kisspeptin-G protein-coupled receptor 54 signaling. *Endocrinology*. 2009;150:2388–2394.
52. **Han SK, Gottsch ML, Lee KJ, et al.** Activation of gonadotropin-releasing hormone neurons by kisspeptin as a neuroendocrine switch for the onset of puberty. *J Neurosci*. 2005;25:11349–11356.
53. **Pelletier G, Liao N, Follea N, Govindan MV.** Mapping of estrogen receptor-producing cells in the rat brain by in situ hybridization. *Neurosci Lett*. 1988;94:23–28.
54. **Qiu J, Bosch MA, Tobias SC, et al.** A G-protein-coupled estrogen receptor is involved in hypothalamic control of energy homeostasis. *J Neurosci*. 2006;26:5649–5655.
55. **Kinoshita M, Tsukamura H, Adachi S, et al.** Involvement of central metastin in the regulation of preovulatory luteinizing hormone surge and estrous cyclicity in female rats. *Endocrinology*. 2005;146:4431–4436.